Controlling IL-7 injections in HIV-infected patients

Chloé Pasin, François Dufour, Laura Villain, Huilong Zhang, Rodolphe Thiébaut

Bull Math Biol manuscript No.
(will be inserted by the editor)

Controlling IL-7 injections in HIV-infected patients

Chloé Pasin · François Dufour · Laura Villain · Huilong Zhang · Rodolphe Thiébaut

Received: date / Accepted: date

Abstract Immune interventions consisting in repeated injections are broadly used as they are thought to improve the quantity and the quality of the immune response. However, they also raise several questions that remain unanswered, in particular the number of injections to make or the delay to respect between different injections to achieve this goal. Practical and financial considerations add constraints to these questions, especially in the framework of human studies. We specifically focus here on the use of interleukin-7 (IL-7) injections in HIV-infected patients under antiretroviral treatment, but still unable to restore normal levels of $CD4^+$ T lymphocytes. Clinical trials have already shown that repeated cycles of injections of IL-7 could help maintaining $CD4^+$ T lymphocytes levels over the limit of 500 cells/μL, by affecting proliferation and survival of $CD4^+$ T cells. We then aim at answering the question : how to maintain a patients level of $CD4^+$ T lymphocytes by using a minimum number of injections (i.e., optimizing the strategy of injections) ? Based on mechanistic models that were previously developed for the dynamics of CD4+ T lymphocytes in this context, we model the process by a piecewise deterministic Markov model. We then address the question by using some recently

C. Pasin · F. Dufour · L. Villain · H. Zhang · R. Thiébaut
Univ. Bordeaux, France

C. Pasin · F. Dufour · L. Villain · H. Zhang · R. Thiébaut
INRIA Bordeaux Sud Ouest, Talence, France

C. Pasin · L. Villain · R. Thiébaut
ISPED, Centre INSERM U1219, 146 rue Léo Saignat, Bordeaux, France
Tel.: +33 5 57 7 13 93, Fax: +33 5 56 24 00 81
E-mail: rodolphe.thiebaut@u-bordeaux.fr

C. Pasin · L. Villain · R. Thiébaut
Vaccine Research Institute VRI, Hôpital Henri Mordor, 51 avenue du Maréchal de Lattre de Tassigny, Créteil, France

F. Dufour
Bordeaux INP, IMB, Bordeaux, France

established theory on impulse control problem in order to develop a numerical tool determining the optimal strategy. Results are obtained on a reduced model, as a proof of concept: the method allows to define an optimal strategy for a given patient. This method could be applied to optimize injections schedules in clinical trials.

Keywords Optimal control · immune therapy · dynamic programming

1 Introduction

The infection by the Human Immunodeficiency Virus (HIV) compromises the immune system functions, mainly because of the depletion of $CD4^+$ T lymphocytes. Combined antiretroviral (cART) therapy has led to a spectacular improvement of patients' survival by controlling virus replication and consequently restoring the immune system functions. However, some patients fail at reconstituting their immune system and recovering normal $CD4^+$ T cell levels, especially when they start antiretroviral treatment late (Lange and Lederman (2003)). Immune therapy has been considered as a complement to cART to help immune restoration. In particular, interleukin-7 (IL-7), a cytokine produced by non-marrow-derived stromal and epithelial cells, is thought to improve thymic production (Mackall et al (2001); Okamoto et al (2002)) and cell survival (Tan et al (2001); Vella et al (1998); Leone et al (2010)). The safety and beneficial effect of injections of exogenous IL-7 was first shown in phase I trials (Sereti et al (2009); Levy et al (2009)) and observational studies (Camargo et al (2009)). Then, phase I/II human clinical trials (INSPIRE 1, 2 and 3 studies) have evaluated the effect of repeated cycles of three IL-7 injections and showed that this therapy helped maintaining HIV infected patients with $CD4^+$ T cells levels above 500 cells/μL (Levy et al (2012)), a level associated with a nearly healthy clinical status (Lewden et al (2007)).

The dynamics of $CD4^+$ T lymphocytes following IL-7 injections can be fitted by mechanistic models based on ordinary differential equations (ODEs). These models contain compartments corresponding to different populations of $CD4^+$ T lymphocytes and biological parameters characterizing these populations. Hence it was possible to quantify the effect of repeated cycles of IL-7 on $CD4^+$ T lymphocytes on specific parameters. Previous work using data from clinical trials (INSPIRE studies) has shown that IL-7 enhances both proliferation and survival of $CD4^+$ T lymphocytes (Thiebaut et al (2014)). Moreover, a differential effect of the injections within a given cycle has been found, the third injection of a cycle appearing to have a weaker effect on proliferation than the first ones (Jarne et al (2017)).

In addition to providing insight into the most important mechanism of the effect of exogenous IL-7, the models have shown a very good predictive capacity (Thiebaut et al (2014); Jarne et al (2017)). Hence, the next step was the determination of the best protocol of injections. A first approach, realized in Jarne et al (2017), consisted in simulating and comparing the regular protocol to three other protocols with different numbers of injections by cycle.

In all four protocols, CD4 counts were measured every three months, and a new cycle was administered when the CD4 numbers were below 550 cells/μL. Comparison was based on three criteria: number of injections received, mean CD4 count and time spent below 500 cells/μL over a four-year period. Results showed that cycles of two injections could be sufficient to maintain CD4 levels, while using less injections than in the clinical protocol. These results suggest the possibility to reduce the number of injections in clinical protocols. However, the three months delay between visits is independent of the patient and constrains the protocol. While some patients with "not too low" baseline CD4 levels could afford coming back later than three months after the last visit, some patients with "low" baseline CD4 levels would need more repeated cycles or more injections by cycle. Individualized protocols could help in achieving the maintenance of the patient's $CD4^+$ T lymphocytes levels over a given threshold by using different patient-dependent timing of injections and doses. The possibility of conducting the lightest intervention for every patient could be very important for the development of IL-7 in HIV infected patients especially for further large clinical trials.

Optimization of schedule and doses is an up-to-date question when working on protocol of injections. In their review on mathematical modeling for immunology, Eftimie et al (2016) emphasize the need for complex optimal control approaches coupled with immunology experiments, in order to improve clinical interventions. Basically, there are two kinds of techniques that can be used to solve optimal control problems: methods involving Pontryagin's maximum principle and dynamic programming approaches. Pontryagin's maximum principle has been applied to a number of biological problems of the form $\frac{dx(t)}{dt} = f(x(t), u(t))$, where the solution to the ordinary differential equation depends on the dynamics of the control function $u(t)$. For example, it was applied to the determination of the optimal schedule of dendritic cells vaccine injection in cancer immunotherapy by Castiglione and Piccoli (2006); Cappuccio et al (2007); Castiglione and Piccoli (2007) and Pappalardo et al (2010). However, in our case, the model is a piecewise deterministic Markov model (PDMP), where dynamics of IL-7 are unknown and not modeled. Addressing the objective of spending the least time possible under the threshold of 500 cells/μL by using repeated injections of IL-7 corresponds in a more formal way to determining actions (injection or not and choice of dose) at given time points over a horizon of time: this can be treated as a problem of impulse control in the optimal control theory. To the best of our knowledge, there is no maximum principle solving this kind of problem. We will focus on a dynamic programming method, as developed in Costa et al (2016). In a formal mathematical framework, we addressed the question of optimizing the schedule of IL-7 injections for a given patient by a two-steps method: determining an adapted mathematical model for the process, and developing a numerical method to determine an optimal strategy of IL-7 injections for a given patient.

As described in Davis (1984), most of the continuous-time stochastic problems of applied probability (including those modeling biological processes) consist of some combination of diffusion, deterministic motion and/or random

jumps. Ordinary differential equations can be included in the class of deterministic motion with random jumps. In our particular framework of modeling cell dynamics after IL-7 injections, jumps correspond to the change of some parameters value. This can be easily and naturally modeled by the largely studied class of Piecewise Deterministic Markov Processes (PDMPs). A non-controlled version of this model can be described by iteration as follows: from a point in the state space, the process follows a deterministic trajectory determined by the flow, until a jump occurs. This jump happens either spontaneously in a random manner, or when the flow hits the boundary of the state space. After the jump, the system restarts from a new point determined by the transition measure of the process. We will show in this article how to model the dynamics of the $CD4^+$ T cells in HIV-infected patients following IL-7 injections using a PDMP.

According to the problem studied in Costa et al (2016), impulse control consists in possible actions only when the process reaches its boundary. This will constitute our framework: the decision maker has the possibility to inject IL-7 when the number of $CD4^+$ T lymphocytes reaches a given level or when a certain amount of time has passed since the last injection. Each action has a cost, and a strategy is defined as the set of all realized actions over a given horizon. The impulse problem consists in determining a strategy of injections minimizing the optimality criterion induced by the cost function. In our case, the cost function depends on the number of injection realized and the time spent with the $CD4^+$ T lymphocytes levels under the threshold of 500 cells/μL, as both quantities should be minimized.

As emphasized by the authors of Dufour et al (2015), the development of computational methods for the control of PDMPs has been limited, and at the moment there is no general method allowing the numerical resolution of optimal control on PDMPs (and in particular impulse control). This constitutes a real challenge. We propose in this work a numerical method based on the results developed in Costa et al (2016). In this paper, the authors studied the existence of a solution of the Bellman-Hamilton-Jacobi equation by showing that the value function is the limit of a sequence of functions given by iteration of an integro-differential operator. This construction leads to a natural method for the computation of the optimal cost and the determination of an optimal strategy of injections. In particular, we have developed an algorithm for the iteration of the operator and applied our numerical tool to the case of the biological model. This provides a proof of concept as it succeeded in determining an optimal strategy for a number of pseudo-patients simulated using previous estimations. The paper is organized as follows: section 2 presents the mathematical modeling of the process, including data and design of INSPIRE studies, as well as mechanistic model and finally the associated PDMP. Section 3 focuses on the optimal control problem, by reminding the main theoretical results from Costa et al (2016) and adapting them to the IL-7 study. Section 4 presents some numerical aspects of the dynamic programming work, necessary to determine the optimal cost function and strategy for a given patient. Results are presented in section 5 and discussion is done in section 6.

2 Mathematical modeling

2.1 Material

Our work is based on three phase I/II multicenter studies assessing the effect of a purified glycosylated recombinant human Interleukin 7 (IL-7) treatment for immune restoration in HIV infected patients under treatment: INSPIRE (Levy et al (2012)), INSPIRE 2 and INSPIRE 3 (Thiébaut et al (2016)). A total of 128 HIV-infected patients under antiretroviral therapy with $CD4^+$ T cell count between 100-400 cells/μL and undetectable viral load for at least 6 months were included among the three studies from the time of the first injection. IL-7 was administered in cycles of weekly injections, with a "complete cycle" defined as three weekly injections. In INSPIRE, all 21 patients received complete cycles of IL-7 at different weight-dependent doses: 10, 20 and 30 μg/kg. In INSPIRE 2 and INSPIRE 3, 23 and 84 patients (respectively) received repeated (and sometimes incomplete) cycles of IL-7 at dose 20 μg/kg. Repeated visits and follow-up once every 3 months after the first cycle allowed to measure biomarkers levels in patients, in particular total $CD4^+$ T cell counts and number of proliferating $CD4^+$ T cells through Ki67 marker. At every visit, a new cycle of injections was administered if the patient's $CD4^+$ T cell level was under 550/μL, in order to globally maintain the levels above 500 cells/μL. The total duration of the studies was 12, 24 and 21 months for INSPIRE, INSPIRE 2 and INSPIRE 3, respectively.

2.2 Mechanistic model

The dynamics of $CD4^+$ T lymphocytes were largely described in Thiebaut et al (2014) and Jarne et al (2017) by using several mechanistic models. We focus here on the following model, described in figure 1: it includes two populations of cells, non-proliferating (or resting, R) and proliferating (P). Resting cells are produced by thymic output at rate λ, become proliferating cells at rate π and die at rate μ_R. Proliferating cells die at rate μ_P and can also divide and produce two non-proliferating cells at rate ρ. The system of differential equations is written as follows :

$$\begin{cases} \dfrac{dR}{dt} = \lambda - \mu_R R - \pi R + 2\rho P \\ \dfrac{dP}{dt} = -\mu_P P - \rho P + \pi R \end{cases} \tag{1}$$

We assume the system is at equilibrium at $t = 0$, before the study begins and any injection is administered. IL-7 injections are realized through cycles containing up to three injections with seven days elapsed between each injection. Parameters estimation was performed using a population approach. Mixed-effect models including intercept, random and fixed effects, were used on log-transformed parameters, in order to both obtain an estimation across

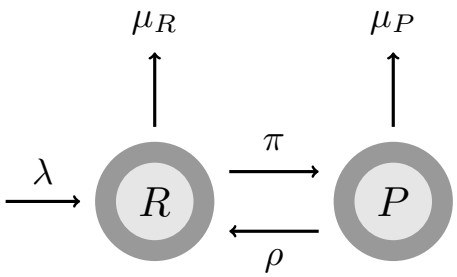

Fig. 1 Mechanistic model for the dynamics of CD4$^+$ T lymphocytes.

population and account for between-individuals variability. In the controlled framework, the decision-maker can decide to inject IL-7 to a patient at a given dose d, and this will affect the value of the proliferation rate π. Each injection denoted by $n \in \{1, 2, 3\}$ of a cycle has a different effect on the value of π for patient i, defined as follows:

$$\tilde{\pi}^i = \tilde{\pi}_0 + \beta_\pi^{(n)} d_i^{0.25} \mathbf{1}_{\{t \in [t^i_{inj}, t^i_{inj} + \tau^i]\}} \tag{2}$$

with $\tilde{\pi} = log(\pi)$; $\beta_\pi = [\beta_\pi^{(1)}, \beta_\pi^{(2)}, \beta_\pi^{(3)}]$ is the vector of effect of each injection of a single cycle; d is the injected dose; t_{inj} is the time (in days) at which IL-7 is injected and τ the length of effect of the injection (in number of days), considered equal to 7 in previous models Jarne et al (2017). Estimation of parameters showed that effect of successive injections on the proliferation rate decreases within a cycle, and in particular the third injection seems to have a much weaker effect (as $\beta_\pi^{(3)} < \beta_\pi^{(2)} < \beta_\pi^{(1)}$) (Jarne et al (2017)).

2.3 Mathematical model: piecewise deterministic Markov process

As described in the introduction, ODEs-based mechanistic models can be included into the broader class of PDMPs. A PDMP is characterized by a state space in which it evolves, a flow, a jump intensity and a measure of transition. From a mathematical point of view, we note X the state space, an open subset of $\mathbb{R}^d$, $d \in \mathbb{N}$, and ∂X its boundary. The flow associated with the process is $\phi(x, t) : \mathbb{R}^d \times \mathbb{R} \mapsto \mathbb{R}^d$. The active boundary is defined as $\Xi = \{x \in \partial X : x = \phi(y, t)\}$ for some $y \in X$ and $t \in \mathbb{R}_+^*$. We will then denote $\overline{X} = X \cup \Xi$ and for $x \in \overline{X}$, we can define $t^*(x) = \inf\{t \in \mathbb{R}_+ : \phi(x, t) \in \Xi\}$. The controlled jump intensity η is a $\mathbb{R}_+$-valued measurable function and determines the law of the stochastic jumps. When the process, i.e. the trajectory of CD4$^+$ T lymphocytes, reaches Ξ, the decision-maker can act by injecting IL-7 to the patient. The action varies according to the dose injected. This leads to a jump in some parameters value, and the process restarts from a new point defined by the transition measure $Q(.|\phi(x_0, \tau), d)$, depending on the dose and the position of the state before the jump $\phi(x_0, \tau)$.

In this section, we present the PDMP associated to the biological process described in section 2.2. Here, the PDMP is patient-dependent. As we focus on the control question (and not the estimation one), we suppose that parameters values of the studied patient are known. Previous work has shown that estimation of ODE's parameters based on population approaches can be reliable (Lavielle and Mentré (2007), Prague et al (2013)). Moreover, the model developed in our particular framework for the CD4 dynamics has shown good predictive abilities (Jarne et al (2017)). Therefore we make the assumption that we determine the strategy for a patient who is already included in a clinical study and for which we had enough observations to estimate its parameters (by running a first cycle of injection for example). As developed in this part, the stochasticity is supposed to be induced by the biological model but not by the uncertainty on the parameters estimation. Sensitivity analysis of the method regarding the estimation uncertainty is provided in Appendix C.

The PDMP modeling the dynamics of $CD4^+$ T lymphocytes of a given patient is defined using six variables: the state vector is denoted by $x = (\gamma, n, \sigma, \theta, p, r)$. γ determines the value of parameter π when combined with n, the number of injections realized in the ongoing cycle. If $d = [d_0, d_1, .., d_{m_d}]$ is the vector of all possibles doses (with $d_0 = 0$), then $\gamma \in \{1..m_d + 1\}$. Injecting dose d_k at the n-th injection of a cycle gives the following: $\gamma(d_k) = k + 1$ and $\pi = \pi_0 + \beta_\pi^{(n)} d(\gamma)^{0.25}$. The two variables σ and θ are time variables, discretized with steps of one day. In particular, σ corresponds to the number of days since the last injection and θ to the running time ($\theta = 1$ at the first injection of the first cycle). Finally, variables p and r are values of compartments P and R solutions of system 1 with parameter π defined by γ and n and other parameters are supposed to have been previously estimated. We suppose the patient is followed until a horizon of time T_h, then the state space is $X = \tilde{X} \cup \Delta$ with

$$\begin{aligned}\tilde{X} = \{1..m_d + 1\} \times \{1..n_{inj}\} \times \{0..T_h - 7(n_{inj} - 1)\} \times \{0..T_h\} \\ \times \{p_{min}..p_{max}\} \times \{r_{min}..r_{max}\}\end{aligned}$$

and Δ is an absorbing state representing the end of the study, at $t = T_h$: $\Delta = (0, 0, 0, T_h, 0, 0)$. For $x = (\gamma, n, \sigma, \theta, p, r) \in X$, the flow is defined as :

- $\phi(x, t) = (\gamma, n, \sigma + t, \theta + t, p, r)$ if $\theta \leq 1$
- $\phi(x, t) = (\gamma, n, \sigma + t, \theta + t, P(t, \gamma, n), R(t, \gamma, n))$ if $\theta \in [1, T_h - 1]$, with $P(t, \gamma, n)$ and $R(t, \gamma, n)$ solutions of system 1 with initial conditions p and r and π determined with γ and n
- $\phi(\Delta, t) = \Delta$

Moreover, even if the deterministic mechanistic model allowed good fits for the data, we make the hypothesis that the process undergoes some stochasticity: in particular, as the value of parameter π is modified by an injection of IL-7 during some days, we suppose that this modification can last randomly up to 7 days after the injection. Stochastic jumps can then occur with intensity η such that for $x \in \tilde{X}$, $\eta(x) = \eta \mathbf{1}_{\{\gamma > 1\}}$ with η a given value and $\eta(\Delta) = 0$. It means that if we consider the modification of π value after an IL-7 injection

through equation 2, τ follows there a random exponential law of parameter η. We define the constant $K = \eta$ such that $\eta(x) \leq K$ for every $x \in \tilde{X}$.

IL-7 injections aim at maintaining the CD4$^+$ T cell level over 500 cells/μL. When this value is reached, we consider that the system has reached a deterministic boundary of the state space. A new injection of IL-7 injection is possible at that moment and gives the possibility to increase CD4$^+$ T cell counts. To account for clinical constraints, we assume a minimum time σ_{min} is observed between the beginning of two consecutive cycles, even if the number of CD4 falls below the threshold of 500. During cycles, the deterministic boundary corresponds to the seven days delay between injections. In a more formal way, the boundary can actually be reached in five different situations described in the following :

- for a technical reason due to the mathematical modeling which cannot account for an impulse action at $t = 0$, we define a first artificial boundary when the study begins, at $\theta = 1 : \Xi_1 = \{x : \theta = 1\}$. This allows a cycle of injections to begin at $\theta = 1$. We suppose the studied patient is already included in the clinical study: it means that its biological parameters are known, and her/his CD4$^+$ T cell count at $t = 0$ as well (either because she/he is at equilibrium, and the values are known from biological parameters, or because some measures have been realized at this time).
- we also define a time corresponding to the end of the study and a boundary when the time reaches the horizon T_h :$\Xi_2 = \{x : \theta \geq T_h\}$
- another boundary is reached when the patient is undergoing a cycle of injections and seven days have passed since the last injection : $\Xi_3 = \{x : n < n_{inj}, \sigma = 7, \theta < T_h\}$
- we also consider a boundary when at least one cycle was already achieved and the count of cells is equal to or below the threshold of 500 cells/μL. We also assume a minimum time σ_{min} is observed between the beginning of two consecutive cycles : $\Xi_4 = \{x : p+r \leq 500, n = n_{inj}, \sigma \geq \sigma_{min}, \theta < T_h\}$
- finally, an artificial boundary is created when π has not returned to its baseline value seven days after the last injection of a cycle : $\Xi_5 = \{x : \gamma > 1, n = n_{inj}, \sigma = 7, \theta < T_h\}$

We define the active boundary as $\Xi = \Xi_1 \cup \Xi_2 \cup \Xi_3 \cup \Xi_4 \cup \Xi_5$. In this process, actions (IL-7 injections) can only be realized when the process hits the active boundary. We model the possibility of not doing an injection in a given cycle by using a fictive dose d_0 equal to zero. When beginning a new cycle of injections, the first injection needs to be positive though. The possible action made by the decision-maker depends on the boundary reached. Therefore for every $x \in \Xi$:

$$A(x) = \begin{cases} \{d_1, ..d_{m_d}\} & \text{if } x \in \Xi_1 \cup \Xi_4 \\ \{0, d_1, ..d_{m_d}\} & \text{if } x \in \Xi_3 \\ \emptyset & \text{if } x \in \Xi_2 \cup \Xi_5 \end{cases}$$

We also define the transition measure (or Kernel): it determines the new point from which the process restarts after a jump. It depends on the injected

dose only when the boundary of the process is reached. All possible situations are the following :

- when the flow hits Ξ_1, the study begins with administration of a cycle of injections. γ takes the value corresponding to the chosen dose. $(p, r) = (P_c, R_c)$, known values from either equilibrium or biological measures made on the patient before the beginning of the study
- when the flow hits Ξ_2, the study is over and nothing happens from absorbing state Δ
- when the flow hits Ξ_3, a new injection is administered to the patient. γ takes the value corresponding to the chosen dose $\gamma(d)$, n increases by one, σ goes back to 0
- when the flow hits Ξ_4, a new cycle of injections begins. γ takes the value corresponding to the chosen dose, n goes back to 1, σ goes back to 0
- when the flow hits Ξ_5, there is no injection. γ goes back to 1
- in case of spontaneous jump, there is no injection and γ goes back to 1

In a formal way, the Kernel Q is written :

$$\begin{aligned} Q(dy|x,d) = {} & \delta_{(\gamma(d),1,0,1,P_c,R_c)}(dy)\mathbf{1}_{\{x\in\Xi_1\}} + \delta_{\Delta}(dy)\mathbf{1}_{\{x\in\Xi_2\}} \\ & + \delta_{(\gamma(d),n+1,0,\theta,p,r)}(dy)\mathbf{1}_{\{x\in\Xi_3\}} + \delta_{(\gamma(d),1,0,\theta,p,r)}(dy)\mathbf{1}_{\{x\in\Xi_4\}} \\ & + \delta_{(1,n,\sigma,\theta,p,r)}(dy)\mathbf{1}_{\{x\in\Xi_5\}} + \delta_{(1,n,\sigma,\theta,p,r)}(dy)\mathbf{1}_{\{x\in\tilde{X}\}} \end{aligned}$$

The impulse control problem consists in determining the optimal scheme of injections and their associated dose according to a given optimality criterion, based on the cost function C: in our case, this cost function depends on the number of injections realized and the time spent with the $CD4^+$ T lymphocytes levels under the threshold of 500 cells/μL. Both quantities need to be minimized, in order to maintain the patient in good health by injecting the least possible. The cost can be divided in two parts. First, the gradual cost penalizes the trajectory of the process through the time spent under the threshold after the beginning of the first cycle. This time is considered in months, approximately, as it is computed as the number of days divided by 30. For $x = (\gamma, n, \sigma, \theta, p, r) \in \tilde{X}$:

$$C^g(x) = \frac{1}{30}\mathbf{1}_{\{p+r<500\}}\mathbf{1}_{\{\theta\geq 1\}}$$

Then, the cost associated to an impulsive action penalizes the fact of injecting IL-7 to the patient :

$$C^i(x,d) = \mathbf{1}_{\{x\in\Xi_1\cup\Xi_4\}} + \mathbf{1}_{\{d\neq 0\}}\mathbf{1}_{\{x\in\Xi_3\}}$$

After the horizon, the cost is null, as $C^i(\Delta) = C^g(\Delta) = 0$.

3 Optimal control

In this section, we will first remind the main theoretical results obtained in Costa et al (2016), then we will transpose these results to our particular context.

3.1 Main theoretical results

The objective of this section is to adapt some results obtained in Costa et al (2016) to our specific context. We follow closely their notation. The set of all realized injections over a given horizon constitutes the strategy of injections. In a more formal way, a strategy u of the decision maker is a sequence $u = \{u_n\}_{n\in\mathbb{N}}$ of functions $u_n : X \mapsto A$ giving the action to realize at punctual time points $t_n \geq 0$ when the system is in state $x \in X$. The set of all admissible strategies is noted $\mathcal{U}$. According to section 2.2 in Costa et al (2016) there exists a continuous-time stochastic process ξ defined on probabilistic space using characteristics ϕ,η and Q depending on the action given by u, such that ξ_t, $t \in \mathbb{R}_+$ corresponds to the state of the variables at time t. To each admissible strategy $u \in \mathcal{U}$, we associate a discounted cost optimality criterion depending on the gradual cost on the trajectory of the process ξ, C^g, and the cost related to an injection, C^i, as defined in section 2.3:

$$\begin{aligned}\mathcal{V}(u, x_0) = \mathbb{E}^u_{x_0}\left[\int_{]0,+\infty[} e^{-\alpha s} C^g(s)ds\right] \\ +\mathbb{E}^u_{x_0}\left[\int_{]0,+\infty[} e^{-\alpha s} I_{\{\xi_{s-}\in\Xi\}} \int_{\mathbf{A}(\xi_{s-})} C^i(\xi_{s-}, a)u(da|s)\mu(ds)\right]\end{aligned} \tag{3}$$

with $\alpha > 0$ the discount factor and where μ is a measure that counts the number of jumps in the process. The impulse control problem aims at finding a strategy u minimizing the discounted cost optimality criterion. Here we want to determine the patient-specific schedule of injections and their dose to optimize the patient's $CD4^+$ T lymphocyte numbers by using a minimum number of injections. The theorem allowing to determine the optimal cost and providing an optimal strategy is adapted from theorem 5.5 in Costa et al (2016). It is stated as followed:

Theorem 1 *Suppose assumptions A, B and C from section 3.2 in Costa et al (2016) are verified. We define the sequence of functions* $\{W_q\}_{q\in\mathbb{N}}$ *for any* $x \in \overline{\mathbf{X}}$ *as follows:*

$$\begin{cases} W_{q+1}(x) = \mathfrak{B}W_q(x) \text{ for } q \in \mathbb{N} \\ W_0(x) = -K_A \mathbf{1}_{A_{\varepsilon_1}}(x) - (K_A + K_B)\mathbf{1}_{A^c_{\varepsilon_1}}(x) \end{cases} \tag{4}$$

with constants K_A *and* K_B *defined as in section 5 of Costa et al (2016),* $A_{\varepsilon_1} = \{x \in \mathbf{X} : t^*(x) > \varepsilon_1\}$ *and*

$$\mathfrak{B}V(y) = \int_{[0,t^*(y)[} e^{-(K+\alpha)t}\mathfrak{R}V(\phi(y,t))dt + e^{-(K+\alpha)t^*(y)}\mathfrak{T}V(\phi(y,t^*(y))) \tag{5}$$

with real-value functions $\mathfrak{R}V$ *and* $\mathfrak{T}V$ *defined for any* V *respectively on* X *and* Ξ *:*

$$\begin{aligned}\mathfrak{R}V(x) &= C^g(x) + qV(x) + \eta V(x) \\ \mathfrak{T}V(z) &= \inf_{d\in\mathbf{A}(z)} \Big\{C^i(z,d) + QV(z,d)\Big\}\end{aligned}$$

q being the signed kernel, which computes the difference between the states before and after the spontaneous jump. For $x \in X$, it is defined with :

$$q(dy|x) = \eta(x)[Q(dy|x) - \delta_x(dy)]$$

The sequence of functions $\{W_q\}_{q\in\mathbb{N}}$ converges to a function W defined on the state space and such that :
i) $W(x_0) = \inf_{u\in\mathcal{U}} \mathcal{V}(u, x_0)$, with $\mathcal{V}$ defined as in equation 3
ii) there is a measurable mapping $\widehat{\varphi} : \Xi \to \mathbf{A}$ such that $\widehat{\varphi}(z) \in \mathbf{A}(z)$ for any $z \in \Xi$ and satisfying

$$C^i(z, \widehat{\varphi}(z)) + QW(z, \widehat{\varphi}(z)) = \inf_{d\in\mathbf{A}(z)} \Big\{C^i(z, d) + QW(z, d)\Big\}. \tag{6}$$

This theorem allows to determine the optimal cost and an optimal injection strategy, consisting in choosing the optimal action $\widehat{\varphi}(z)$ for every point $z \in \Xi$ reached on the trajectory of the process. Indeed, the iteration of the sequence $\{W_q\}_{q\in\mathbb{N}}$ defined by equation 4 can be realized by numerically approximating the operator $\mathfrak{B}$ defined in equation 5. This will give an approximation of the function W, and in particular of $W(x_0)$, corresponding to the optimal cost. Moreover, to obtain an optimal strategy, the process is the following: we simulate a trajectory from x_0, then when a boundary is reached, the chosen action corresponds to the one minimizing the criterion $C^i(z, d) + QW(z, d)$, as given by equation 6.

3.2 Application

The process describing the effect of IL-7 on CD4$^+$ T lymphocytes dynamics is now well defined by its characteristics ϕ, η and Q, boundaries and possible actions in section 2.3. Moreover, both gradual cost on the trajectory and impulse cost were defined in that section. We will quickly describe in this part how to apply the results from theorem 1 for our specific problem, i.e. determining the function $\mathfrak{B}$ needed for the computation of the optimal strategy. For a more detailed and formal computation, we refer the reader to appendix A. We need to compute:

$$\mathfrak{B}V(y) = \int_{[0,t^*(y)[} e^{-(K+\alpha)t}\mathfrak{R}V(\phi(y,t))dt + e^{-(K+\alpha)t^*(y)}\mathfrak{T}V(\phi(y,t^*(y)))$$

We define

$$G(V, y) = \int_{[0,t^*(y)[} e^{-(K+\alpha)t}\mathfrak{R}V(\phi(y,t))dt \tag{7}$$

and

$$H(V, y) = e^{-(K+\alpha)t^*(y)}\mathfrak{T}V(\phi(y,t^*(y)) \tag{8}$$

We define a time interval Δt (in practice equal to one day) and for every $y = (\gamma, n, \sigma, \theta, p, r) \in \tilde{X}$, we note

$$n^*(y) = \left\lfloor \frac{t^*(y)}{\Delta t} \right\rfloor$$

For every $j \in \{0..n^*(y)-1\}$, we denote $\phi_j(y,t) = \phi(y, j\Delta t)$ and $\phi(y,t^*(y)) = (\gamma, n, \sigma + t^*(y), \theta + t^*(y), p^*(y), r^*(y))$. The integral defined in equation 7 is computed by approximation using the classic trapezoidal rule using the $j\Delta t$ nodes. Thus, $G(V,y)$ can be approximated by a linear combination of $\{V(y_j)\}_{j\in\{0..n^*(y)-1\}}$, with y_j depending on $\phi_j(y,t)$. Moreover, $H(V,y)$ is proportional to $V(\overline{y})$, with $\overline{y}$ depending on the boundary reached in $\phi(y,t^*(y))$. Finally, for every point $y \in \tilde{X}$, if we note $\overline{y} = y_{n^*(y)}$, $\mathfrak{B}V(y)$ can be computed as a linear combination of $\{V(y_j)\}_{j\in\{0..n^*(y)\}}$.

4 Numerical aspects of the dynamic programming method

From theorem 1 we know that we need to compute the sequence $\{W_q\}_{q\in\mathbb{N}}$ such that for $y \in \overline{\mathbf{X}}$, $W_0(y) = -K_A \mathbf{1}_{A_{\varepsilon_1}}(y) - (K_A + K_B)\mathbf{1}_{A^c_{\varepsilon_1}}(y)$ and $W_{q+1}(y) = \mathfrak{B}W_q(y)$ for $q \in \mathbb{N}$. The sequence converges to a function W defined on $\overline{\mathbf{X}}$ that allows the determination of the optimal cost and the optimal protocol of injections achieving that cost. This computation is realized on a grid of the state space: at each iteration q, a new matrix is computed, each element on line v and column s corresponding to $\mathfrak{B}W_q(x_{vs})$, with x_{vs} element of the grid Γ of the state space. The implementation of our algorithm was realized in Matlab version R2016b (The MathWorks, Inc., Natick MA, USA, 1984). In this section, we give elements to understand how the method is implemented. The structure of the code is detailed in Appendix B.

4.1 Discretization of the state space

The grid Γ contains points of the form $(\gamma, n, \sigma, \theta, p, r)$. γ and n are discrete variables with $\gamma \in \{1...m_d + 1\}$, $n \in \{1..n_{inj}\}$. σ and θ are discretized with a time step of one day, with $\sigma \in \{0..\sigma_{\max}\}$ and $\theta \in \{0..T_h\}$. Solutions p and r of the ODE system are continuous and are discretized in a regular grid, with $p \in \{p_{\min}..p_{\max}\}$ with regular step h_p and $r \in \{r_{\min}..r_{\max}\}$ with regular step h_r. We then obtain :

$$n_p = \frac{p_{\max} - p_{\min}}{h_p} + 1$$

$$n_r = \frac{r_{\max} - r_{\min}}{h_r} + 1$$

h_r and h_p are chosen such that both n_p, $n_r \in \mathbb{N}$ count the number of values of p and r on the grid, respectively.

4.2 Organization of the grid

We arrange all points of the grid Γ in a matrix M of size $N_{sum} \times N_{pr}$, with N_{sum} corresponding to the number of possible $(\gamma, n, \sigma, \theta)$ combinations and

$N_{pr} = n_p n_r$ number of possible (p, r) combinations. Each element $M(v,s)_{\substack{v\in\{1..N_{sum}\}\\ s\in\{1..N_{pr}\}}}$ corresponds to a given combination $(\gamma, n, \sigma, \theta, p, r)$ of Γ, through the following bijection :

$$\begin{aligned}\chi\colon\ & \Gamma \to \{1..N_{sum}\} \times \{1..N_{pr}\} \\ & x_{vs} = (\gamma, n, \sigma, \theta, p, r) \mapsto (v, s) = \Big(\chi_l(\gamma, n, \sigma, \theta), \chi_c(p, r)\Big)\end{aligned}$$

χ_l is defined in the following way : v corresponds to a given value of $(\gamma, n, \sigma, \theta)$. Possible combinations of (σ, θ) depend on the value of (γ, n): for example, during the first cycle, when $n = 1$, $\sigma = 0$ is associated with $\theta = 1$, while when $n = 2$, $\sigma = 0$ is associated with $\theta = 8$. We divide the lines of matrix M by defining then $N_{\gamma n} = (m_d + 1)n_{inj}$ blocks, corresponding to the possible combinations of (γ, n). Each block is indexed by $i = f(\gamma, n) = \gamma + (m_d+1)(n-1) \in \{1..N_{\gamma n}\}$ and contains combinations of (σ, θ), indexed by $j = g_i(\sigma, \theta) \in \{1..N_{b_i}\}$ within the i-th block. The total number of lines of matrix M is the sum of the number of lines in each block: $N_{sum} = \sum_{i=1}^{N_{\gamma n}} N_{b_i}$. We can define a vector $l_{block} = (1, 1 + N_{b_1}, .., 1 + \sum_{i=1}^{k} N_{b_i}, .., \sum_{i=1}^{N_{\gamma n}-1} N_{b_i})$ of length $N_{\gamma n}$, that determines the index of the first line of each block. Finally :

$$v = \chi_l(\gamma, n, \sigma, \theta) = l_{block}(i) + j - 1$$

with $i = f(\gamma, n)$ and $j = g_i(\sigma, \theta)$. χ_c is defined in the following way :

$$s = \chi_c(p, r) = \frac{p - p_{\min}}{h_p} + 1 + n_p \frac{r - r_{\min}}{h_r}$$

such that $s = 1$ when $(p, r) = (p_{\min}, r_{\min})$ and $s = n_p n_r$ when $(p, r) = (p_{\max}, r_{\max})$.

4.3 Iteration of the algorithm

Each iteration of the algorithm computes then a matrix M_q such that

$$M_q(v, s) = W_q\Big(M(v, s)\Big) = W_q(x_{vs})$$

For every $x = (\gamma, n, \sigma, \theta, p, r) \in \Gamma$, $W_q(x)$ is a linear combination of some $W_q(x_m)$, $m \in \{1..M_x\}$, as shown in equation 12 from appendix A. Values of $W_q(x_m)$ are given by $M_q(\chi(x_m))$; they are linearly combined and implemented in $M_{q+1}(\chi(x))$.

4.4 Convergence criterium

We assume that the sequence converges when $\|W_{q+1} - W_q\|_\infty < \epsilon$. In practice, we compute $\max_{v,s} |M_{q+1}(v, s) - M_q(v, s)|$ and we consider that the sequence converges with $\epsilon = 0.001$. It usually occurs after 35 to 45 iterations.

5 Results

We applied the previously described method to the model detailed in section 2.3, with a choice of $m_d = 2$ possibles doses: $d = [0, 10, 20]$ (unit = μg/kg), cycles of 3 injections: $n_{inj} = 3$ and a reduced horizon $T_h = 365$ days. We also assumed a minimum time of $\sigma_{\min} = 30$ days between the end of a cycle and the beginning of a new one. For a given patient with fixed biological parameters, we can approximate the function W in a grid of the state space through convergence of the sequence $\{W_q\}$: this determines the optimal cost over all strategies. Moreover, using equation 6 from theorem 1, we can simulate the strategy choosing the optimal action to realize when reaching the boundary of the state space and compute the cost of the obtained strategy. As some randomness is included in the model by the time of effect of an injection of parameter π, we simulate $N = 5000$ realizations of a protocol on a given patient with a Monte Carlo method and compute the expectation of its cost. From that, we check the numeric performance of our method by first comparing the cost of the optimal strategy to the computation of the optimal cost from the value function W. Moreover, we wish to compare the optimal strategy to other "naive" protocols. For each protocol, including the optimal one, we compute by Monte Carlo the mean cost, the standard deviation and the minimum cost achievable. This is usually reached when the patient responds well to all injections, i.e. the effect of the injection on parameter π lasts 7 days after every injection. In order to compare protocols based on clinical criteria, we also computed by Monte Carlo the mean number of CD4+ T cells count until horizon, the mean time spent under 500 cells/μL (in days) and the mean number of injections over all simulations. These comparisons were realized with 50 pseudo-patients. Parameters values were generated from the posterior law estimated on real data from INSPIRE trials in Thiébaut et al (2016). Patients are divided in three categories according to their initial levels of $CD4^+$ T cells: "very low" baseline ($100 - 200$ cells/μL), "low" baseline ($200 - 300$ cells/μL) and "not too low" baseline ($300 - 400$ cells/μL). Table 1 sums up the characteristics of the pseudo-patients population.

We first compare the value of the optimal function obtained from the numerical computation of W with the cost of the optimal strategy. For a sake of clarity, we show detailed results in table 2 only for three chosen patients. Patient A is in category "very low", patient B in category "low" and patient C in category "very low". We note that for these 3 patients the two cost values are very similar, meaning that we make a good approximation of the value function with our numerical method. We make the same observation on the 47 other patients (data not shown). Also of note is the hierarchy of the cost between the categories of patients. Very low patients have higher optimal costs (between 8.4 and 12) than low (between 3.9 and 9.4) and not too low (between 2.1 and 4.2). This is consistent with the fact that the lower baseline CD4 levels the patient has, the more time will be spent under 500 cells/ μL and the more injections are needed, which both increase the cost of the strategy of injections.

Table 1 Characteristics of the pseudo-patients population.

Parameter	Mean (std)
λ (cells/day)	2.24 (0.39)
ρ (/day)	1.96 (0.84)
π_0 (/day)	0.0461 (0.0035)
μ_R (/day)	0.0503 (0.0033)
μ_P (/day)	0.0717 (0.014)
β_{π_1}	0.958
β_{π_2}	0.752
β_{π_3}	0.143
Category	Number of patients (%)
Very low	4 (8%)
Low	24 (48%)
Not too low	22 (44%)

Table 2 Comparison of cost values from value function and Monte Carlo simulation. Std = standard deviation.

	Patient A very low	Patient B low	Patient C not too low
Optimal cost $W(x_0)$	9.47	6.11	2.87
Cost of optimal strategy : mean (std) (obtained by Monte Carlo)	9.53 (0.85)	6.20 (0.56)	2.90 (0.36)

We also realized comparisons of several protocols. We simulated five "naive" protocols : P1 with 3-injections cycles, P2 with a first cycle of 3 injections then 2-injections cycles, P3 with 2-injections cycles, P4 with a first cycle of 2 injections then 1-injection cycles and P5 with 1-injection cycles, all protocols with dose 20. Assessing the cost of these protocols is interesting as they imply variable trajectories within the same patient as well as different values for clinical criteria. Moreover they would be clinically feasible and represent a good basis for comparison for our optimal strategy. For every protocol k, we note $\mathcal{P}_{+k}$ the space of patients such that cost of optimal strategy is lower than cost of protocol k and n_{+k} its size. We have computed the mean relative positive variation of cost value (MRC), as shown in table 3. We note C_{opt_i} the mean cost of optimal strategy for patient i and C_{Pk_i} the mean cost of protocol k for patient i. The MRC allows computing the mean percentage of gain in term of cost function when using the optimal strategy over protocol k:

$$MRC_k = \frac{1}{n_{+k}} \sum_{i \in \mathcal{P}_{+k}} \frac{(C_{Pk_i} - C_{opt_i})}{C_{Pk_i}} \tag{9}$$

Results show that mean cost of the optimal strategy is always lower than all other simulated strategies (except one patient for protocol 4, but this is due to numerical approximation, as for this patient $W(x_0)$=4.0, C_{opt} = 4.1 and

Table 3 Computation of the mean relative variation of cost value (MRC) for every protocol allows determining the mean percentage of gain in term of cost function when using the optimal strategy over protocol k. P1: cycles of 3 injections. P2: first cycle of 3 injections then cycles of 2 injections. P3: cycles of 2 injections. P4: first cycle of 2 injections then cycles of 1 injection. P5: cycles of 1 injection.

Protocol	P1	P2	P3	P4	P5
n_+	50	50	50	49	50
MRC	43%	31%	20%	5.7%	8.8%

C_{P_4}=4.0). The percentage of cost reduction of the optimal strategy compared to the other protocols in the simulated population of pseudo patients varies from 5.7 to 43%. It confirms that our numerical method allows optimizing the cost function.

In addition to comparing the cost value of all five protocols to the optimal strategy, we have also compared clinical criteria such as the mean number of CD4+ T cells count until horizon, the mean time spent under 500 cells/μL (in days) and the mean number of injections over all simulations. Results of these comparisons are shown in figure 5, where each point corresponds to the value of the criterion for one pseudo-patient, and each color corresponds to the category of the patients ("very low", "low" and "not too low" baseline). We observe that mean cost of the optimal strategy is lower than other simulated protocols and the optimal strategy achieves a good balance between all clinical criteria. Even if CD4+ T cells levels are not as high as for protocols P1, P2 and P3, the optimal strategy allows to spend as much time with levels over 500 cells/μL as these protocols by using less injections. Protocol P5 has the same performance as the optimal strategy for "not too low" patients, as these strategies are very often the same on these patients. The same observation is made on protocol P4 and the "low" patients. Overall, figure 5 shows that the determined strategy allows optimization of the cost function through the chosen criteria (time spent under 500 and number of injections).

More detailed results of comparison of cost function and clinical criteria between optimal strategy and protocols Pk are displayed in table 4 for patients A, B and C. For these three patients, we observe again that mean cost of the optimal strategy is lower than all other simulated strategies. For patient A, the optimal strategy is achieved by two first cycles of two injections then cycles of one injection. For patient B, the optimal strategy consists in a first cycle of 2 injections followed by 1-injection cycles. We can see that the minimum cost is the same for the optimal strategy and protocol P3 (= 5.91): when the patient has a good response to all injections, these strategies are the same. For patient C, the optimal strategy is obtained with 1-injection cycles. Similarly, the minimum cost is the same for the optimal strategy and protocol P5 (= 2.79). For all patients, the optimal strategy is very intuitive: the first complete cycles are needed to raise the number of CD4 over 500 cells/ μL; then, 1-injection cycles allow to sustain the levels over 500 cells/ μL. For "not too low" patients, CD4 levels are high enough to use only one injection in the first cycle. This helps reducing the number of injections: in patient A, the optimal

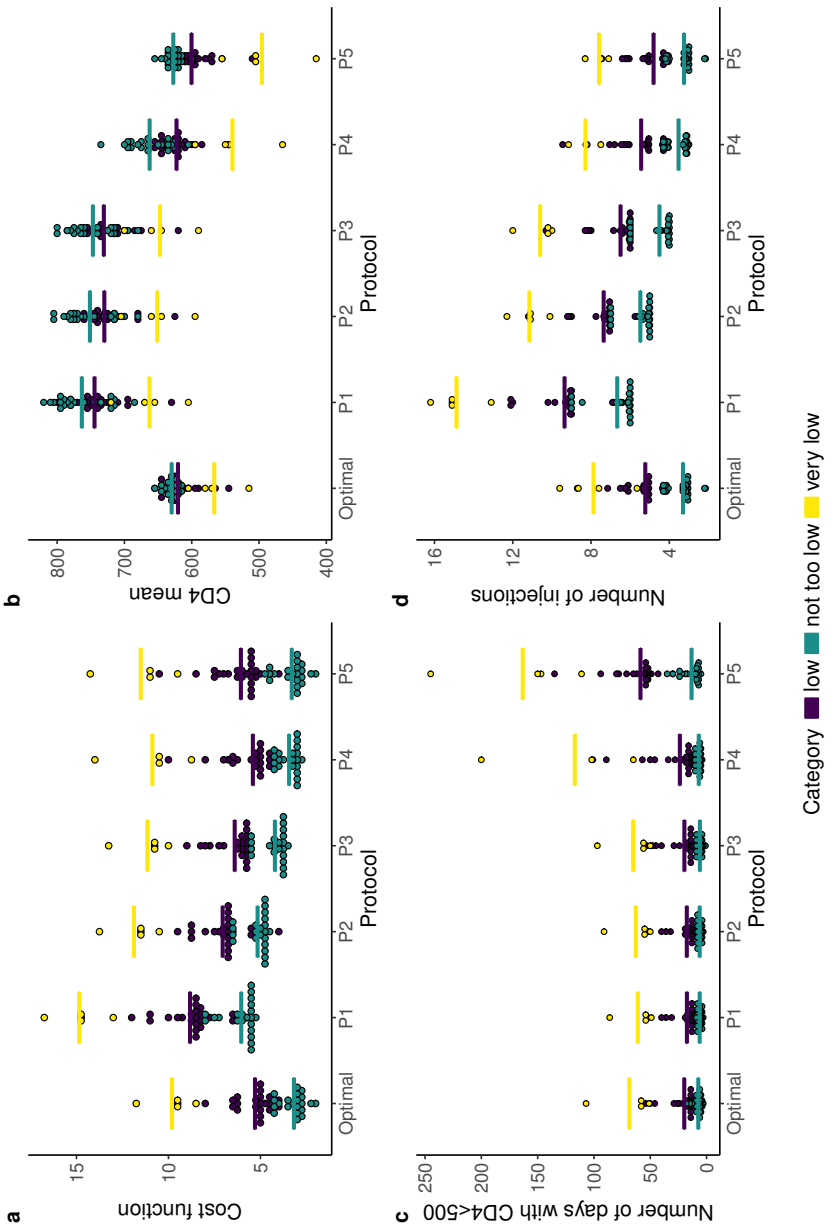

Fig. 2 Comparison of cost (3a) and clinical criteria (3b : mean number of CD4+ T cells count until horizon, 3c : mean time spent under 500 cells/μL in days, 3d : mean number of injections over all simulations) between the determined optimal strategy and the five other protocols. Each point corresponds to the value of a pseudo patient, with "very low" patients in yellow, "low" in purple and "not too low" in blue. Mean values within each category are represented by horizontal colored lines. P1: cycles of 3 injections. P2: first cycle of 3 injections then cycles of 2 injections. P3: cycles of 2 injections. P4: first cycle of 2 injections then cycles of 1 injection. P5: cycles of 1 injection.

Table 4 Comparison of protocols of injections for patient A, B and C. P1: cycles of 3 injections. P2: first cycle of 3 injections then cycles of 2 injections. P3: cycles of 2 injections. P4: first cycle of 2 injections then cycles of 1 injection. P5: cycles of 1 injection.

Protocol	P1	P2	P3	P4	P5	Optimal
Patient A						
Mean cost	14.8	11.6	10.7	10.4	11.1	9.53
Std	0.52	0.62	0.68	1.21	1.23	0.85
Min cost	14.6	11.4	10.4	9.56	10.1	8.82
CD4 mean	671	662	659	552	506	578
Days under 500	54.5	55.4	56.5	102	150	58.0
Number of injections	15.1	11.1	10.2	8.25	7.48	8.66
Patient B						
Mean cost	9.35	7.62	6.91	6.26	6.63	6.20
Std	1.14	1.00	0.98	0.70	0.87	0.56
Min cost	8.62	6.91	6.14	5.91	6.12	5.91
CD4 mean	762	742	736	622	598	625
Days under 500	18.4	19.0	24.2	28.1	61.9	24.4
Number of injections	9.83	7.73	6.84	6.05	5.27	6.10
Patient C						
Mean cost	5.54	4.75	3.80	3.08	2.93	2.90
Std	0.29	0.24	0.31	0.37	0.49	0.36
Min cost	5.46	4.70	3.73	2.95	2.79	2.79
CD4 mean	774	762	758	666	631	631
Days under 500	5.56	5.53	5.65	5.90	8.43	5.89
Number of injections	6.02	5.02	4.04	3.13	3.03	3.07

strategy requires 2 to 7 less injections than P1, P2 and P3 but allows to spend as much time over 500 cells/ μL. In patient C the optimal strategy requires one less injection as P3 but allows to spend as much time over 500 cells/ μL. It can be noted that a third injection is never used, even for the first cycles of very low patient. It is due to our choice of cost function: it balances the number of injections and the number of months spent under 500 cells/ μL. The effect of a third injection is usually too low to allow increasing the time spent over 500 cells/ μL by one month and is then not chosen as part of the optimal strategy. These results suggest that our numerical method allows to determine an optimal strategy of injections, and the clinical interpretation of the results are consistent with the mathematical method.

In term of trajectories of the process, figures 3a and 3b show some trajectories obtained with respectively the 2-injection cycles protocol (P3) and the optimal strategy for patient A. We can note that even if $CD4^+$ levels are globally lower in the optimal strategy compared to the two-injections cycles at dose 20 μg/kg, it still allows a maintenance over the threshold of 500 cells/μL

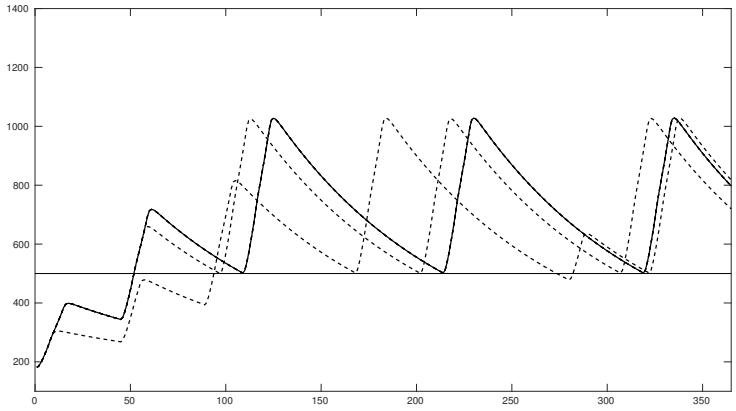

(a) Dynamics of $CD4^+$ T lymphocytes in patient A under P3, a 2-injections cycles protocol (dose 20).

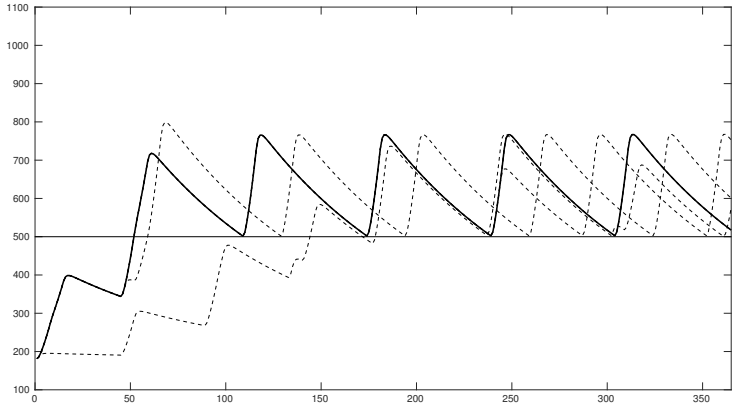

(b) Dynamics of $CD4^+$ T lymphocytes in patient A under the determined optimal strategy.

Fig. 3 Dynamics of $CD4^+$ T lymphocytes in patient A. Straight line corresponds to the "best" outcome, i.e., when the effect of all injections lasts seven days. Dashed line corresponds to other possible trajectories, when this effect can last less than seven days.

by using less injections: indeed, in the best case scenario, the 2-injections cycle strategy implies 5 cycles of 2 injections which is a total of 10 injections, while the optimal strategy induces 2 cycles of 2 injections and 4 single injections, which is a total of 8 injections. The trajectories for patients B and C are provided in appendix D. All together, our results support the interest of determining the optimal strategy based on a criterion combining both the number of injections and the time spent under 500.

6 Discussion

In this work, we have developed a numerical tool allowing to solve an impulse control problem for a PDMP. The specificity of our work is in the development of a dynamic programming method in the context of a specific biological framework. The objective is to determine the optimal strategy of IL-7 injections for a given HIV-infected patient, in order to maintain $CD4^+$ T lymphocytes levels over the threshold of 500 cells/μL. We first modeled the dynamics of $CD4^+$ T lymphocytes during repeated cycles of IL-7 injections by a PDMP. Then, we solved the impulse control problem by iterating a sequence defined by an integro-differential operator. Theoretical results have shown that this sequence converges to the value function, which allows to determine the optimal action that should be realized at every point of the boundary. We proposed a numerical tool approximating the sequence and the value function on a grid of the state space and applied it to our clinical question. As our method relies on numerical approximation, the obtained optimal strategy could be an approximation of the theoretical one. However the obtained results suggest that we managed to determine optimal strategies for pseudo-patients and that our method allows improving the strategy of injections. Although the horizon of study is only one year, these results are also consistent with a clinical interpretation. The optimal strategy determined for different patients is indeed intuitive: the first cycles aim at increasing the $CD4^+$ T lymphocytes levels and should contain as many injections as possible until the levels are acceptable. Then, the following cycles sustain the CD4 levels over the threshold, and punctual injections are sufficient to reach this objective. The optimal strategy, determined with our method, has a lower cost than other possible clinical strategies. Actually, the obtained optimal strategy depends on the cost previously defined, and we could explore other optimal strategies depending on other cost functions. For example, it could be interesting to use different weights on the time spent under 500 cells /μL and the number of injections (depending on the clinician priorities), or to account for the possible negative side effects due to higher doses (this would need additional data on the question). Finally, the model could be extended by studying the patient until a longer horizon (up to two years). This rises the issue of the increase of computational time (by increasing the size of the grid of the state space) and constitutes a new challenge in itself. In the end, we hope to use this tool in future possible clinical trial investigating the effect of IL-7 injections with patients-specific schedules of injections, personalized and optimized using this method.

Acknowledgements We would like to thank the main investigators and supervisors of INSPIRE 2 and 3 studies: Jean-Pierre Routy, Irini Sereti, Margaret Fischl, Prudence Ive, Roberto F. Speck, Gianpiero D'Ozi, Salvatore Casari, Sharne Foulkes, Ven Natarajan, Guiseppe Tambussi, Michael M. Lederman, Therese Croughs and Jean-François Delfraissy. This work was supported by the Investissements d'Avenir program managed by the ANR under reference ANR-10-LABX-77.

References

Camargo JF, Kulkarni H, Agan BK, Gaitan AA, Beachy LA, Srinivas S, He W, Anderson S, Marconi VC, Dolan MJ, et al (2009) Responsiveness of t cells to interleukin-7 is associated with higher cd4+ t cell counts in hiv-1–positive individuals with highly active antiretroviral therapy–induced viral load suppression. The Journal of infectious diseases 199(12):1872–1882

Cappuccio A, Castiglione F, Piccoli B (2007) Determination of the optimal therapeutic protocols in cancer immunotherapy. Mathematical biosciences 209(1):1–13

Castiglione F, Piccoli B (2006) Optimal control in a model of dendritic cell transfection cancer immunotherapy. Bulletin of mathematical biology 68(2):255–274

Castiglione F, Piccoli B (2007) Cancer immunotherapy, mathematical modeling and optimal control. Journal of theoretical Biology 247(4):723–732

Costa O, Dufour F, Piunovskiy A (2016) Constrained and unconstrained optimal discounted control of piecewise deterministic markov processes. SIAM Journal on Control and Optimization 54(3):1444–1474

Davis MH (1984) Piecewise-deterministic markov processes: A general class of non-diffusion stochastic models. Journal of the Royal Statistical Society Series B (Methodological) pp 353–388

Dufour F, Zhang H, et al (2015) Numerical methods for simulation and optimization of piecewise deterministic markov processes. John Wiley & Sons

Eftimie R, Gillard JJ, Cantrell DA (2016) Mathematical models for immunology: Current state of the art and future research directions. Bulletin of mathematical biology 78(10):2091–2134

Jarne A, Commenges D, Villain L, Prague M, Lévy Y, Thiébaut R, et al (2017) Modeling $cd4^+$ t cells dynamics in hiv-infected patients receiving repeated cycles of exogenous interleukin 7. The Annals of Applied Statistics 11(3):1593–1616

Lange CG, Lederman MM (2003) Immune reconstitution with antiretroviral therapies in chronic hiv-1 infection. Journal of Antimicrobial Chemotherapy 51(1):1–4

Lavielle M, Mentré F (2007) Estimation of population pharmacokinetic parameters of saquinavir in hiv patients with the monolix software. Journal of pharmacokinetics and pharmacodynamics 34(2):229–249

Leone A, Rohankhedkar M, Okoye A, Legasse A, Axthelm MK, Villinger F, Piatak M, Lifson JD, Assouline B, Morre M, et al (2010) Increased cd4+ t cell levels during il-7 administration of antiretroviral therapy-treated simian immunodeficiency virus-positive macaques are not dependent on strong proliferative responses. The Journal of Immunology 185(3):1650–1659

Levy Y, Lacabaratz C, Weiss L, Viard JP, Goujard C, Lelièvre JD, Boué F, Molina JM, Rouzioux C, Avettand-Fénoêl V, et al (2009) Enhanced t cell recovery in hiv-1–infected adults through il-7 treatment. The Journal of clinical investigation 119(4):997

Levy Y, Sereti I, Tambussi G, Routy J, Lelievre J, Delfraissy J, Molina J, Fischl M, Goujard C, Rodriguez B, et al (2012) Effects of recombinant human interleukin 7 on t-cell recovery and thymic output in hiv-infected patients receiving antiretroviral therapy: results of a phase i/iia randomized, placebo-controlled, multicenter study. Clinical Infectious Diseases 55(2):291–300

Lewden C, Chêne G, Morlat P, Raffi F, Dupon M, Dellamonica P, Pellegrin JL, Katlama C, Dabis F, Leport C, et al (2007) Hiv-infected adults with a cd4 cell count greater than 500 cells/mm3 on long-term combination antiretroviral therapy reach same mortality rates as the general population. JAIDS Journal of Acquired Immune Deficiency Syndromes 46(1):72–77

Mackall CL, Fry TJ, Bare C, Morgan P, Galbraith A, Gress RE (2001) Il-7 increases both thymic-dependent and thymic-independent t-cell regeneration after bone marrow transplantation. Blood 97(5):1491–1497

Okamoto Y, Douek DC, McFarland RD, Koup RA (2002) Effects of exogenous interleukin-7 on human thymus function. Blood 99(8):2851–2858

Pappalardo F, Pennisi M, Castiglione F, Motta S (2010) Vaccine protocols optimization: in silico experiences. Biotechnology advances 28(1):82–93

Prague M, Commenges D, Guedj J, Drylewicz J, Thiébaut R (2013) Nimrod: A program for inference via a normal approximation of the posterior in models with random effects based on ordinary differential equations. Computer methods and programs in biomedicine 111(2):447–458

Sereti I, Dunham RM, Spritzler J, Aga E, Proschan MA, Medvik K, Battaglia CA, Landay AL, Pahwa S, Fischl MA, et al (2009) Il-7 administration drives t cell–cycle entry and expansion in hiv-1 infection. Blood 113(25):6304–6314

Tan JT, Dudl E, LeRoy E, Murray R, Sprent J, Weinberg KI, Surh CD (2001) Il-7 is critical for homeostatic proliferation and survival of naive t cells. Proceedings of the National Academy of Sciences 98(15):8732–8737

Thiebaut R, Drylewicz J, Prague M, Lacabaratz C, Beq S, Jarne A, Croughs T, Sekaly RP, Lederman MM, Sereti I, et al (2014) Quantifying and predicting the effect of exogenous interleukin-7 on cd4+ t cells in hiv-1 infection. PLoS Comput Biol 10(5):e1003,630

Thiébaut R, Jarne A, Routy JP, Sereti I, Fischl M, Ive P, Speck RF, D'offizi G, Casari S, Commenges D, et al (2016) Repeated cycles of recombinant human interleukin 7 in hiv-infected patients with low cd4 t-cell reconstitution on antiretroviral therapy: results of 2 phase ii multicenter studies. Clinical Infectious Diseases 62(9):1178–1185

Vella AT, Dow S, Potter TA, Kappler J, Marrack P (1998) Cytokine-induced survival of activated t cells in vitro and in vivo. Proceedings of the National Academy of Sciences 95(7):3810–3815

A Optimal control : application

We defined the process describing the effect of IL-7 on $CD4^+$ T lymphocytes dynamics by its characteristics ϕ, η and Q, boundaries and possible actions in section 2.3. We also defined both gradual cost on the trajectory and impulse cost in that section. As we aim at

applying the results from theorem 1 to determine the optimal cost and an optimal strategy by dynamic programming, we need to determine how to compute numerically the function $\mathfrak{B}$ to iterate the sequence $\{W_q\}_{q\in\mathbb{N}}$ defined in equation 4. As a reminder, $\mathfrak{B}$ is defined in Costa et al (2016) by :

$$\mathfrak{B}V(y) = \int_{[0,t^*(y)[} e^{-(K+\alpha)t}\mathfrak{R}V(\phi(y,t))dt + e^{-(K+\alpha)t^*(y)}\mathfrak{T}V(\phi(y,t^*(y)))$$

We will first detail the computation of $\mathfrak{R}$ then $\mathfrak{T}$, and we will finally show how to compute $\mathfrak{B}$.

Computation of $\mathfrak{R}$

For $x = (\gamma, n, \sigma, \theta, p, r) \in X$, and function $V : \overline{X} \to \mathbb{R}$, $\mathfrak{R}$ is defined as :

$$\mathfrak{R}V(x) = C^g(x) + qV(x) + \eta V(x)$$

with q computing the difference between the states before and after the spontaneous jump. As Q depends on the action only when the process hits the active boundary,

$$\begin{aligned} q(dy|x,d) &= \eta(x)[Q(dy|x) - \delta_x(dy)] \\ &= \mathbf{1}_{\{\gamma>1\}}\eta[\delta_{(1,n,\sigma,\theta,p,r)}(dy) - \delta_{(\gamma,n,\sigma,\theta,p,r)}(dy)] \end{aligned}$$

then for every function V, and as $K = \eta$:

$$\begin{aligned} qV(x) &= \int V(y)q(dy|x) \\ &= \mathbf{1}_{\{\gamma>1\}}K[V(1,n,\sigma,\theta,p,r) - V(\gamma,n,\sigma,\theta,p,r)] \end{aligned}$$

Then

$$\begin{aligned} \mathfrak{R}V(x) &= \frac{1}{30}\mathbf{1}_{\{p+r\leq 500\}} + qV(x) + KV(x) \\ &= \frac{1}{30}\mathbf{1}_{\{p+r\leq 500\}} + KV(1,n,\sigma,\theta,p,r)\mathbf{1}_{\{\gamma>1\}} + KV(x)\mathbf{1}_{\{\gamma=1\}} \end{aligned}$$

Finally,

$$\begin{aligned} \mathfrak{R}V(x) &= \frac{1}{30}\mathbf{1}_{\{p+r\leq 500\}} + KV(1,n,\sigma,\theta,p,r) \\ \mathfrak{R}V(\Delta) &= KV(\Delta) \end{aligned} \tag{10}$$

Computation of $\mathfrak{T}$

For $x \in \Xi$, and function $V : \overline{X} \to \mathbb{R}$, $\mathfrak{T}$ is defined as :

$$\begin{aligned} \mathfrak{T}V(x) &= \inf_{d\in A(x)} \Big\{C^i(x,d) + QV(x,d)\Big\} \\ &= \inf_{d\in A(x)} \Big\{\mathbf{1}_{x\in\Xi_1\cup\Xi_4} + \mathbf{1}_{d\neq 0}1_{x\in\Xi_3} + \int V(y)\Big[\delta_{(\gamma(d),1,0,1,P_c,R_c)}(dy)\mathbf{1}_{\{x\in\Xi_1\}} \\ &\quad +\delta_\Delta(dy)\mathbf{1}_{\{x\in\Xi_2\}} + \delta_{(\gamma(d),n+1,0,\theta,p,r)}(dy)\mathbf{1}_{\{x\in\Xi_3\}} + \delta_{(\gamma(d),1,0,\theta,p,r)}(dy)\mathbf{1}_{\{x\in\Xi_4\}} \\ &\quad +\delta_{(1,n,\sigma,\theta,p,r)}(dy)\mathbf{1}_{\{x\in\Xi_5\}}\Big]\Big\} \end{aligned}$$

Finally,

$$\begin{aligned} \mathfrak{T}V(x) &= \inf_{d\in A(x)} \Big\{[1 + V(\gamma(d),1,0,1,P_c,R_c)]\mathbf{1}_{x\in\Xi_1} \\ &\quad +[\mathbf{1}_{d\neq 0} + V(\gamma(d),n+1,0,\theta,p,r)]\mathbf{1}_{x\in\Xi_3} \\ &\quad +[1 + V(\gamma(d),1,0,\theta,p,r)]\mathbf{1}_{x\in\Xi_4}\Big\} + V(\Delta)\mathbf{1}_{x\in\Xi_2} + V(1,n,\sigma,\theta,p,r)\mathbf{1}_{x\in\Xi_5} \\ \mathfrak{T}V(\Delta) &= V(\Delta) \end{aligned} \tag{11}$$

Computation of $\mathfrak{B}$

Now, for $Y \in \overline{X}$, and function $V : \overline{X} \to \mathbb{R}$, we need to compute :

$$\mathfrak{B}V(y) = \int_{[0,t^*(y)[} e^{-(K+\alpha)t}\mathfrak{R}V(\phi(y,t))dt + e^{-(K+\alpha)t^*(y)}\mathfrak{T}V(\phi(y,t^*(y)))$$

As we cannot make an exact computation of $\mathfrak{B}V$ on $\overline{X}$, we need to approximate this computation on a grid of the state space. In order to detail the approximation of the computation, we define

$$G(V,y) = \int_{[0,t^*(y)[} e^{-(K+\alpha)t}\mathfrak{R}V(\phi(y,t))dt$$

and

$$H(V,y) = e^{-(K+\alpha)t^*(y)}\mathfrak{T}V(\phi(y,t^*(y))$$

as in 7 and 8. We define a time interval Δt (in practice equal to one day) and for every $y = (\gamma, n, \sigma, \theta, p, r) \in \tilde{X}$, we note

$$n^*(y) = \left\lfloor \frac{t^*(y)}{\Delta t} \right\rfloor$$

For every $j \in \{0..n^*(y)-1\}$, we note $\phi_j(y,t) = \phi(y, j\Delta t)$ and $\phi(y,t^*(y)) = (\gamma, n, \sigma+t^*(y), \theta+t^*(y), p^*(y), r^*(y))$. The integral defined in equation 7 is computed by approximation using the classic trapezoidal rule using the $j\Delta t$ nodes :

$$\begin{aligned} G(V,y) \simeq\ & \frac{\Delta t}{2}\mathfrak{R}V(y) + \frac{\Delta t}{2}e^{-(K+\alpha)t^*(y)}\mathfrak{R}V(\phi(y,t^*(y))) \\ & + \sum_{j=1}^{n^*(y)-2} \Delta t e^{-(K+\alpha)j\Delta t}\mathfrak{R}V(\phi_j(y,t)) \end{aligned}$$

with $\mathfrak{R}V(x) = \frac{1}{30}\mathbf{1}_{\{p+r\leq 500\}} + KV(1,n,\sigma,\theta,p,r)$, as computed in 10. Then we obtain the following for every $y = (\gamma, n, \sigma, \theta, p, r) \in \tilde{X}$:

$$\begin{aligned} G(V,y) =\ & \frac{\Delta t}{2}\left(\frac{1}{30}\mathbf{1}_{\{p+r<500\}} + KV(1,n,\sigma,\theta,p,r)\right) \\ & + \frac{\Delta t}{2}e^{-(K+\alpha)t^*(y)}\left(\frac{1}{30}\mathbf{1}_{\{p^*+r^*<500\}} + KV(1,n,\sigma+t^*,\theta+t^*,p^*(y),r^*(y))\right) \\ & + \Delta t \sum_{j=1}^{n^*(y)-2} e^{-(K+\alpha)j\Delta t}\left(\frac{1}{30}\mathbf{1}_{\{p_j+r_j<500\}} + KV(1,n,\sigma+j\Delta t,\theta+j\Delta t,p_j,r_j)\right) \end{aligned}$$

Now, we need to compute H as defined in 8 : it depends on $\mathfrak{T}V(\phi(y,t^*(y)))$, which takes different values according to the boundary reached in that point, as written in equation 11. Moreover, as we know the flow, we can give conditions on $y = (\gamma, n, \sigma, \theta, p, r)$ to reach a given boundary in $\phi(y,t^*(y))$. Then :

- if $\phi(y,t^*(y)) \in \Xi_1$ $(\theta \leq 1)$ then

$$H(V,y) = \inf_{d\in[d_1,..d_{m_d}]} \left\{ e^{-(K+\alpha)t^*(y)}\left[1 + V(\gamma(d),1,0,1,P_c,R_c)\right]\right\}$$

- if $\phi(y,t^*(y)) \in \Xi_2$ $(\theta + t^*(y) \geq T_h)$ then

$$H(V,y) = e^{-(K+\alpha)t^*(y)}V(\Delta)$$

- if $\phi(y,t^*(y)) \in \Xi_3$ $(n < n_{inj}, \theta + t^*(y) < T_h)$ then

$$\begin{aligned} H(V,y) =\ & \inf_{d\in[0,d_1,..d_{m_d}]} \left\{ e^{-(K+\alpha)t^*(y)}\left[\mathbf{1}_{\{d\neq 0\}}\right.\right. \\ & \left.\left. + V(\gamma(d), n+1, 0, \theta+t^*(y), p^*(y), r^*(y))\right]\right\} \end{aligned}$$

– if $\phi(y,t^*(y)) \in \Xi_4$ $(n = n_{inj}, \gamma = 1, \theta + t^*(y) < T_h)$ then

$$H(V,y) = \inf_{d\in[d_1,..d_{m_d}]} \Big\{ e^{-(K+\alpha)t^*(y)} \Big[1 + V(\gamma(d), 1, 0, \theta + t^*(y), p^*(y), r^*(y)) \Big] \Big\}$$

– if $\phi(y,t^*(y)) \in \Xi_5$ $(n = n_{inj}, \gamma > 1, \theta + t^*(y) < T_h)$ then

$$H(V,y) = e^{-(K+\alpha)t^*(y)} V(1, n, \sigma + t^*(y), \theta + t^*(y), p^*(y), r^*(y))$$

Finally, for every $y = (\gamma, n, \sigma, \theta, p, r) \in \tilde{X}$:

$$\begin{aligned}
\mathfrak{B}V\ (y) = {} & \frac{\Delta t}{2}\Big(\frac{1}{30}\mathbf{1}_{\{p+r<500\}} + KV(1,n,\sigma,\theta,p,r)\Big) \\
& + \tfrac{\Delta t}{2} e^{-(K+\alpha)t^*(y)} \Big[\frac{1}{30}\mathbf{1}_{\{p^*+r^*<500\}} + KV(1,n,\sigma+t^*,\theta+t^*,p^*(y),r^*(y)) \Big] \\
& + \Delta t \sum_{j=1}^{n^*(y)-2} e^{-(K+\alpha)j\Delta t} \Big[\frac{1}{30}\mathbf{1}_{\{p_j+r_j<500\}} + KV(1,n,\sigma+j\Delta t,\theta+j\Delta t,p_j,r_j) \Big] \\
& + \inf_{d\in[d_1,..d_{m_d}]} \Big\{ e^{-(K+\alpha)t^*(y)} \Big[1 + V(\gamma(d),1,0,1,P_c,R_c) \Big] \Big\} \mathbf{1}_{\{\theta\le 1\}} \\
& + e^{-(K+\alpha)t^*(y)} V(\Delta) \mathbf{1}_{\{\theta + t^*(y) \ge T_h\}} \\
& + \inf_{d\in[0,d_1,..d_{m_d}]} \Big\{ e^{-(K+\alpha)t^*(y)} \Big[\mathbf{1}_{\{d\neq 0\}} \\
& + V(\gamma(d), n+1, 0, \theta + t^*(y), p^*(y), r^*(y)) \Big] \Big\} \mathbf{1}_{\{n<n_{inj}, \theta + t^*(y) < T_h\}} \\
& + \inf_{d\in[d_1,..d_{m_d}]} \Big\{ e^{-(K+\alpha)t^*(y)} \Big[1 \\
& + V(\gamma(d), 1, 0, \theta + t^*(y), p^*(y), r^*(y)) \Big] \Big\} \mathbf{1}_{\{n=n_{inj}, \gamma=1, \theta + t^*(y) < T_h\}} \\
& + e^{-(K+\alpha)t^*(y)} V(1, n, \sigma + t^*(y), \theta + t^*(y), p^*(y), r^*(y)) \mathbf{1}_{\{n=n_{inj}, \gamma>1, \theta + t^*(y) < T_h\}}
\end{aligned} \tag{12}$$

and

$$\mathfrak{B}V(\Delta) = \int_{[0,+\infty)} e^{-(K+\alpha)t} KV(\Delta) dt = \frac{K}{K+\alpha} V(\Delta)$$

B Structure of the code

Structure of the code and its subroutines are shown in figure 4. Application in the results section requires the following grid :

– $\gamma \in \{1..3\}$
– n $\in \{1..3\}$
– $\sigma \in \{0..351\}$
– $\theta \in \{1..365\}$
– $p \in \{2..110\}$ depending on the patient
– $r \in \{100..1500\}$ depending on the patient

The grid of the state space created in Matlab contains 67614 lines and 7755 columns. For a given patient, the computation of 40 iterations of the sequence (convergence is reached between 35 and 45 iterations) requires between 5 and 6 days.

C Sensitivity analysis of the method

To evaluate how the uncertainty on individual parameters estimation could impact the determination of the optimal strategy, we have realized a sensitivity analysis. For a given patient, we suppose a normal distribution of parameters λ and ρ. We generate $L = 500$ pairs of parameters (λ, ρ) from this joint distribution. Each pair corresponds to an initial

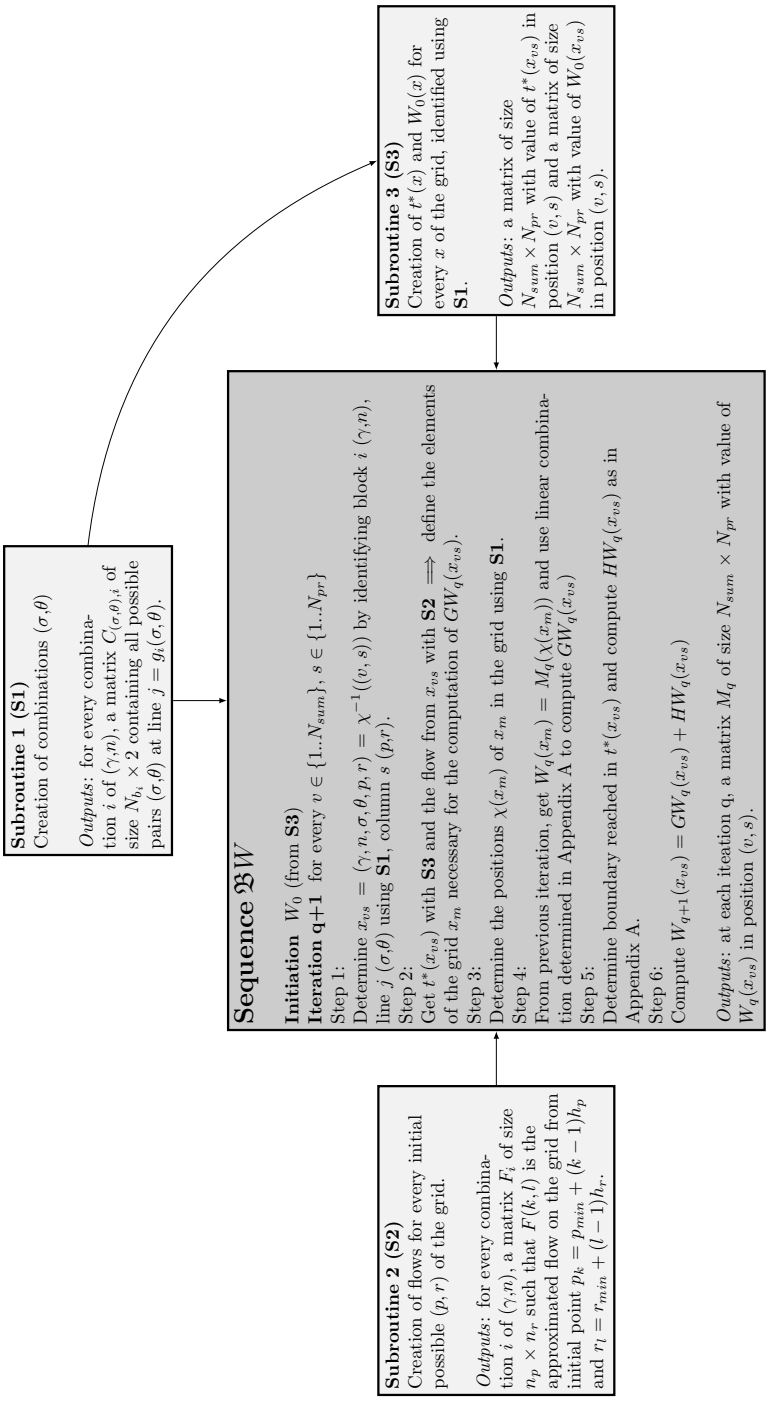

Fig. 4 Structure of the code and its subroutines.

Table 5 Pairs of (λ,ρ), associated CD4 values and mean cost for protocols P1 to P5. P1: cycles of 3 injections. P2: first cycle of 3 injections then cycles of 2 injections. P3: cycles of 2 injections. P4: first cycle of 2 injections then cycles of 1 injection. P5: cycles of 1 injection. P4 is the optimal protocol for mean value of (λ,ρ).

Category	λ	ρ	$CD4_0$	P1	P2	P3	P4	P5
Mean	2.065	2.022	289	6.55	5.54	5.54	**4.16**	4.95
Q1	1.506	2.305	224	8.59	6.94	6.03	**5.20**	5.67
Q1	2.062	1.180	223	11.6	9.19	8.52	**7.28**	8.02
Q1	1.701	1.747	224	8.94	7.31	6.50	**5.60**	6.40
Q1	2.163	1.078	222	11.9	9.50	8.82	**8.04**	8.39
Q1	1.737	1.371	224	9.06	7.39	6.64	**5.71**	6.48
Q1	1.689	1.758	223	8.92	7.31	6.52	**5.62**	6.40
Q1	1.728	1.689	224	9.00	7.35	6.63	**5.71**	6.45
Q1	1.426	2.599	222	8.54	6.90	5.98	**5.14**	5.62
Q1	2.493	0.838	222	13.3	11.0	10.3	**8.85**	9.76
Q1	1.805	1.542	223	9.23	7.59	6.94	**6.36**	6.66
Q3	2.160	2.594	337	5.62	4.81	3.88	3.15	**3.04**
Q3	2.424	1.956	336	5.83	4.99	4.10	3.81	**3.21**
Q3	2.638	1.625	335	6.10	5.22	4.30	3.93	**3.31**
Q3	2.219	2.429	337	5.68	4.85	3.93	3.21	**3.11**
Q3	2.477	1.879	337	5.87	5.04	4.12	3.83	**3.21**
Q3	2.466	1.896	337	5.86	5.01	4.09	3.82	**3.22**

value of lymphocytes T $CD4_0$. We determine the empirical quartiles of the distribution of the $CD4_0$ and focus on the pairs inducing values close the first and the third quartiles. Then, for each pair we simulate the five possible protocols P1 to P5 and compare them to the optimal strategy determined on the mean value of (λ,ρ). In practice, values of pairs and associated values of CD4 are displayed in table 5. For the mean value of (λ,ρ), we determined the optimal strategy to be a first cycle of 2 injections and then cycles of 1 injection, which corresponds to protocol P4. We show in table 5 the cost of each protocol for each pair of (λ,ρ), and we put in bold the minimum cost over the five protocols. We can see that protocol P4 achieves the minimum cost for all pairs inducing CD4 values at the first quartile. For pairs inducing CD4 values at the third quartile, the protocol achieving the minimum cost is P5. However, the difference of cost is not huge and P4 actually induces more time spent over the 500 threshold and less than one more injection than P5 on average, which is still acceptable. Overall, this shows that even with some error on the estimation on λ, ρ we would be able to determine a strategy achieving a good balance between clinical criteria.

D Trajectories of patients B and C

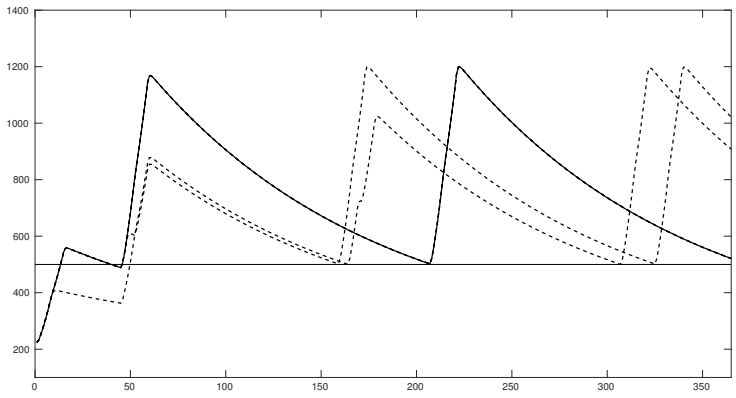

(a) Dynamics of $CD4^+$ T lymphocytes in patient B under P3, a 2-injections cycles protocol (dose 20).

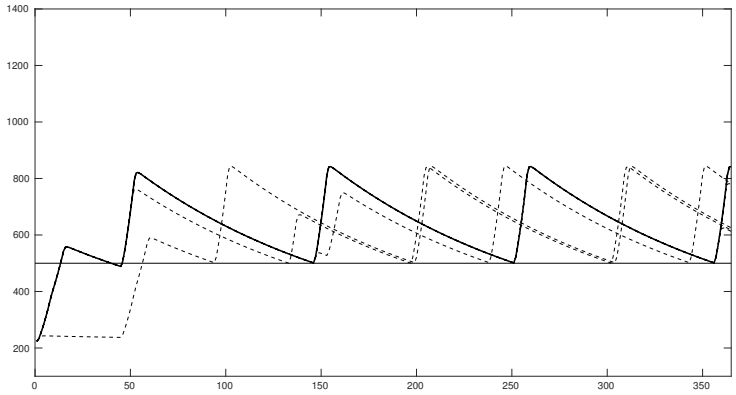

(b) Dynamics of $CD4^+$ T lymphocytes in patient B under the determined optimal strategy.

Fig. 5 Dynamics of $CD4^+$ T lymphocytes in patient B. Straight line corresponds to the "best" outcome, i.e., when the effect of all injections lasts seven days. Dashed line corresponds to other possible trajectories, when this effect can last less than seven days.

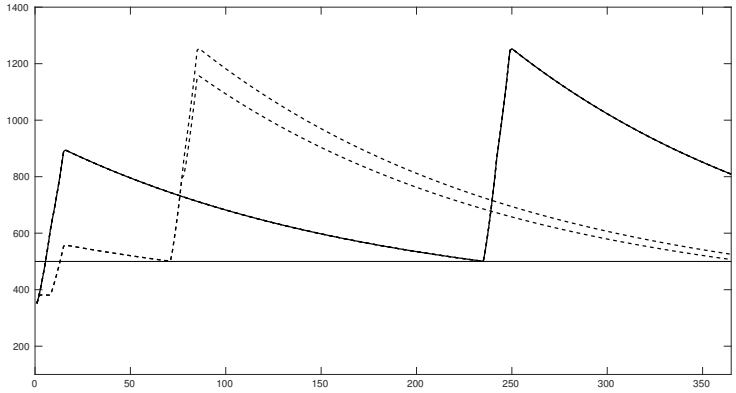

(a) Dynamics of $CD4^+$ T lymphocytes in patient C under P3, a 2-injections cycles protocol (dose 20).

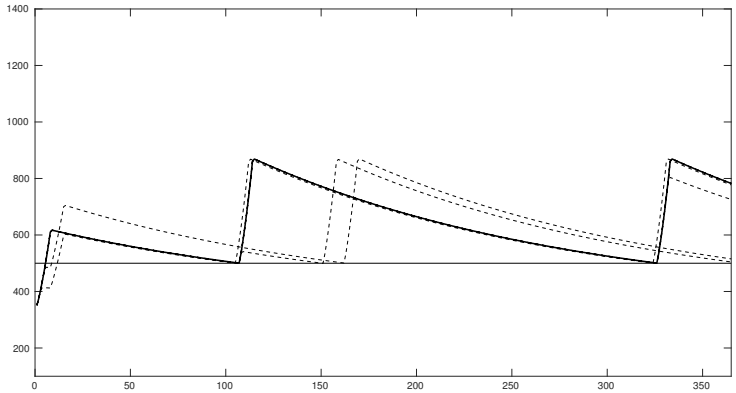

(b) Dynamics of $CD4^+$ T lymphocytes in patient C under the determined optimal strategy.

Fig. 6 Dynamics of $CD4^+$ T lymphocytes in patient C. Straight line corresponds to the "best" outcome, i.e., when the effect of all injections lasts seven days. Dashed line corresponds to other possible trajectories, when this effect can last less than seven days.